Desalination and Water Treatment
www.deswater.com

doi: 10.5004/dwt.2020.25825

193 (2020) 152–158
July

Removal of phosphate ions from polluted water using a hybrid anion exchanger

Abdallah Said Battah[a], Ragaa El-Sheikh Shohaib[b], Mohammed Gammal Abdelwahed[b], Hesham Abdelhamid Ezzeldin[a], Mohamed E.A. Ali[a,c,*]

[a]*Hydrogeochemistry Department, Desert Research Centre, Cairo 11753, Egypt, Tel. +201144098296; email: m7983ali@gmail.com (M. El-Sayed), Tel. +201060917699; email: battahbattah1992@hotmail.com (A.S. Battah), Tel. +201009452081; email: h.ezzeldin@hotmail.com (H.A. Ezzeldin)*
[b]*Chemistry Department, Faculty of Science, Zagazig University, Zagazig, Egypt, Tel. +201222180577; email: ragaaelsheikh@hotmail.com (R. El-Sheikh Shohaib), Tel. +201223168235; email: abdelwahed49@hotmail.com (M.G. Abdelwahed)*
[c]*Egypt Desalination Research Center of Excellence (EDRC), Desert Research Center*

Received 9 March 2020: Accepted 6 April 2020

ABSTRACT

Pollution of water resources with phosphate due to industrial activities restricts water usage for different purposes. This work depends on the collection of some surface and groundwater samples from the fertilizer industrial effluent of Helwan, Egypt, then analyzed for the determination of major and minor constituents. Based on the chemical analyses, it was found that some water samples contain higher concentrations of phosphate. Therefore, a new hybrid anion exchanger (HAEX) for selective sorption of phosphate from polluted water was prepared. Durability, mechanical strength, and high sorption affinity of hydrated ferric oxide toward phosphate urged us to use it along with HAEX as a good adsorbent. The prepared ion exchanger was characterized using Fourier transform-infrared spectroscopy, X-ray diffraction, and scanning electron microscopy to confirm the chemical structure and surface morphology. The results show that the exchanger had high selectivity for the removal of phosphate from higher concentrations of competing for sulfate, chloride, and bicarbonate anions. The removal percentage was 100% after 2 h due to the combined presence of Coulombic and Lewis acid–base interactions.

Keywords: Amberlite; Ferric oxide; Selectivity; Phosphate removal; Polluted water

1. Introduction

There are many technologies for wastewater treatment, among them ion exchange, reverse osmosis, membrane distillation, and photocatalysis [1]. For the advantages of ion exchange resins such as the absence of sludge, less labor-intensive and lower overall operation cost have made it the most common method for wastewater treatment [2], Polymeric materials offer durability and preferred mechanical strength. The used Amberlite MB9L is a mixed ion exchanger, its matrix is styrene-divinylbenzene and ethylstyrene copolymer with functional groups of trimethylamine quaternized, hydroxide (Anion part) and sulfonated hydrogen form (Cation part) as shown in Fig. 1c. Earlier research works at Lehigh University led to the development of polymeric ligand exchangers (PLEs) that exhibit high phosphate selectivity over competing for sulfate and chloride ions [3–5]. PLEs are also amenable to efficient regeneration and reuse. Extensive researches were undertaken to explore the effectiveness of fixed-bed processes for phosphate removal because of their operational simplicity and adaptability to change wastewater flow rates and compositions [6]. However, the inorganic metal oxide particles (e.g. Fe) lack the mechanical strength and attrition resistance properties for prolonged operation in

* Corresponding author.

Presented at the 4th International Water Desalination Conference: Future of Water Desalination in Egypt and the Middle East, 24–27 February 2020, Cairo, Egypt

fixed-bed units [7]. Oxides of polyvalent metals, namely, Fe(III), Ti(IV), Zr(IV) exhibit very favorable ligand sorption properties through the formation of inner-sphere complexes [7–10]. For example hydrated Fe(III) oxide (HFO) is innocuous, inexpensive, readily available, and chemically stable over a wide pH range. Recently, however, it was shown that the ligand sorption capacity can be increased by dispersing HFO nanoparticles within polymeric anion exchangers [11]. Dispersing HFO nanoparticles within an anion exchanger is scientifically challenging because both ferric ion (Fe^{3+}) and quaternary ammonium groups (R_4N^+) in an anion exchange resin are positively charged. Amberlite resin and modified Amberlite were used for pollutant removal with high efficiency [12]. The work aims to modify the commercial Amberlite resin by nano hydrated ferric oxide in order to make it highly selective for phosphate ions.

2. Materials and methods

2.1. Materials

The used resin is a mixed ion exchange resin called Amberlite MB9L, available from Rohm and Haas Company. $KMnO_4$, $FeSO_4$, and acetone from Sigma-Aldrich (USA) were also used.

2.2. Preparation of adsorbents

The composite was prepared according to previous work in a batch method [13]. In brief, 10 g of Amberlite resin was oxidized using 1,300 ml of potassium permanganate (600 mg/L) with stirring for 30 min. The formed intermediate was rinsed twice with deionized water, and then was immersed in 330 ml of 5% (w/v) ferrous sulfate solution and shaken for 4 h. After that, the hybrid resin was excessively rinsed with deionized water. These steps were repeated for a second and third cycle of iron loading. Afterward, the hybrid resin was rinsed with deionized water and acetone, and then dried in an oven at 35°C for 12 h. When the Amberlite resin, without any modifications, was added to a mixture containing different ions, it showed no selectivity, as shown in Table 1. The excess of sulfate ions, as a result of rinsing in ferrous sulfate solution, was washed out with a 0.5 M NaOH solution.

Table 1
Adding the resin (AMBERLITE MB9L) only before modification to the mixture (no selectivity)

	Before (ppm)	After (ppm)	Efficiency %
F	9	0	100
Cl	65.2	1.2	98.2
Br	16.8	0	100
NO_2	9.7	0	100
NO_3	3.5	0.085	97.6
PO_4	62	0	100
SO_4	36.3	0	100
Fe	77.89	29.66	61.9
Cu	102.3	0.43	99.6
Mn	96.65	1.13	98.8
Pb	102.3	0.77	99.2

2.3. Characterization

Fourier transform infrared spectrophotometer (FT-IR) (Bruker Vertex 70 FT-IR spectrometer model), scanning electron microscopy (SEM, EO FESEM 1530), X-ray diffraction (XRD; Bruker-AXS D8 Discover diffractometer, Co-Ka source) and energy-dispersive X-ray spectroscopy (EDX) analysis were carried out for adsorbent identification.

2.4. Batch adsorption experiment

A solution containing different concentrations of (F^-, Cl^-, Br^-, PO_4^{-3}, SO_4^{-2}, NO_2^-, NO_3^-, Fe, Cu, Mn, Pb) species was prepared for identifying the selectivity of the modified resin; a stock of PO_4^{-3} was also prepared. All batch adsorption experiments were performed on a mechanical shaker with a shaking speed of 200 rpm. The concentrations were monitored using an inductively coupled plasma (ICP) spectrophotometer (Thermo Jarrell Ash; Model: ICP 61E) and ion chromatography (ICS-3000 Reagent-Free IC System) for anion concentrations determination. To study the effect of adsorption time, 0.5 g of modified resin was shaken in 50 ml of a solution containing ppm of PO_4^{-3} at different time intervals (5, 10, 30, 40, 50, 60, 70, 80, 90, 120, 150, and 180 min.). The effect of the adsorbate solution temperature was investigated by shaking 0.5 g of adsorbent with 50 ml of phosphate solution at 25°C, 40°C, and 60°C. After each adsorption process, the solution was filtrated and taken to ion chromatography (IC system) for analysis. The adsorption capacity was calculated according to the following equation:

$$q = \frac{\left(C_i - C_f\right)V}{m} \tag{1}$$

The removal % of PO_4^{-3} was calculated as follows:

$$\% = \frac{\left(C_i - C_f\right)}{C_i} \times 100 \tag{2}$$

where "q" is the adsorption capacity (mg/g), C_i and C_f are the initial and the final PO_4^{-3} concentration, respectively, in (mg/L), V is the volume of the adsorbate solution (in liters), and m is the mass of adsorbent (in g).

2.5. Reusability of the adsorbent

Reusability of the adsorbent was carried out by washing it with a single solution containing 2% NaOH and 2% NaCl, then washed with DI water several times. Afterward, the adsorbent was used again and the adsorption and removal of phosphate were calculated according to the previous equations.

3. Results and discussions

3.1. Effect of the adsorbent modification

By adding a commercial Amberlite resin to a polluted water sample, complete ions removal occurs indicating

no selectivity (Table 1). Despite the newly modified resin showed high selectivity toward phosphate ion removal, an increment of some other ions such as iron and sulfate occurred, (Table 2). Such problems were overcome by increasing the concentration of the permanganate to allow much more iron oxidation. The modified resin was then washed with 0.5M NaOH solution for excess sulfate removal. The newly modified resin was tested with a naturally-occurring polluted water sample and the concentration of the different ions were observed, (Table 3). The selectivity toward phosphate removal, without any additional increase of the other ion concentration, was observed. Fig. 1 shows that there is a change of the external color of Amberlite after modification with ferric oxide, where the yellow spherical beads were changed to brown color without any change in its original spherical shape. The FT-IR spectra of the adsorbent before and after the loading of ferric oxide was illustrated in Fig. 2. The figure showed that the commercial or non-modified Amberlite resin (Fig. 2a) exhibited a broad peak at 3,392 cm^{-1}, which can be assigned to O–H stretching vibration of the hydroxyl group [14,15]. Meanwhile, two peaks at about 2,924 and 2,359 cm^{-1} indicating C–H stretching of the aromatic ring of polystyrene-divinylbenzene matrix in anion resin [15]. Furthermore, a peak at 1,417 cm^{-1} corresponds to C–H bending of the quaternary ammonium functional group of ion resin [16]. As shown in Fig. 2b, the peak pattern of FO-Amberlite is similar to Amberlite resin, an additional peak observed at 550 cm^{-1} is attributed to Fe–O stretching vibration which clearly indicated loading of ferric oxide onto Amberlite [17]. Fig. 3 shows the X-ray diffraction (XRD) patterns of Amberlite before and after modification. As shown in Fig. 3b, six characteristic peaks for nano iron oxide (2θ = 36.417, 43.353, 45.425, 50.459, 52.3, 61.249) were identified. These peaks are in agreement with the database of standard nano iron oxide (ASTM Card No: 86-1359) [18–20]. Scanning electron microscopy (SEM) image of the non-modified Amberlite resin (Fig. 3c) showed the uniform

Table 2
After modification the resin

Species	Before (ppm)	After (ppm)	Efficiency %
F	9	6.3	30
Cl	65.2	55	15.6
Br	16.8	0	100
NO_2	9.7	3.4	64.9
NO_3	3.5	1.5	57
PO_4	62	0	100
SO_4	36.3	131	–
Fe	77.89	144.2	–
Cu	102.3	31.35	69.3
Mn	96.65	34.75	64
Pb	102.3	10.67	89.58

Table 3
After increasing the concentration of permanganate and washing by NaOH (0.5 M)

Species	Before (ppm)	After (ppm)	Efficiency%
F	9	6.3	30
Cl	65.2	55	15.6
Br	16.8	0	100
NO_2	9.7	3.4	64.9
NO_3	3.5	1.5	57.1
PO_4	62	0	100
SO_4	60	58	3
Fe	77.89	0.5841	99.3
Cu	102.3	0.48	99.5
Mn	96.65	14.88	84.6
Pb	102.3	0.16	99.8

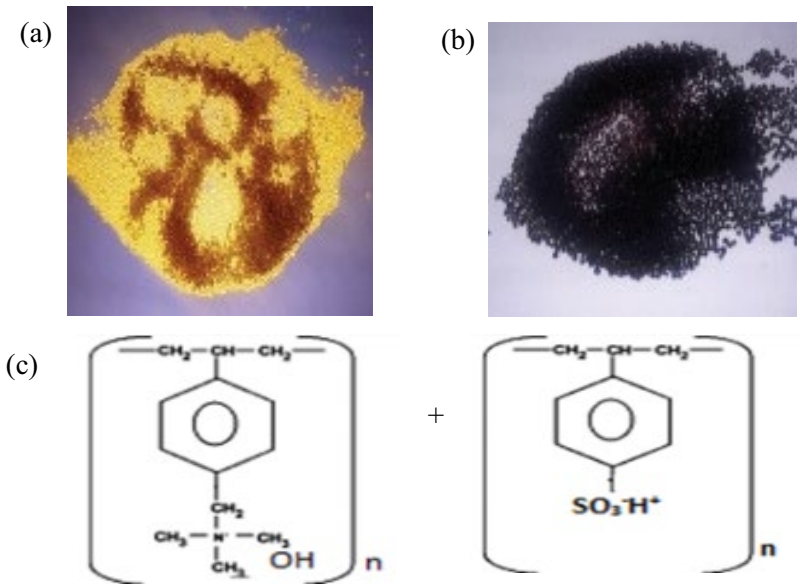

Fig. 1. (a) Shape of Amberlite MB9L, (b) shape of modified resin, and (c) chemical structure of Amberlite MB9L.

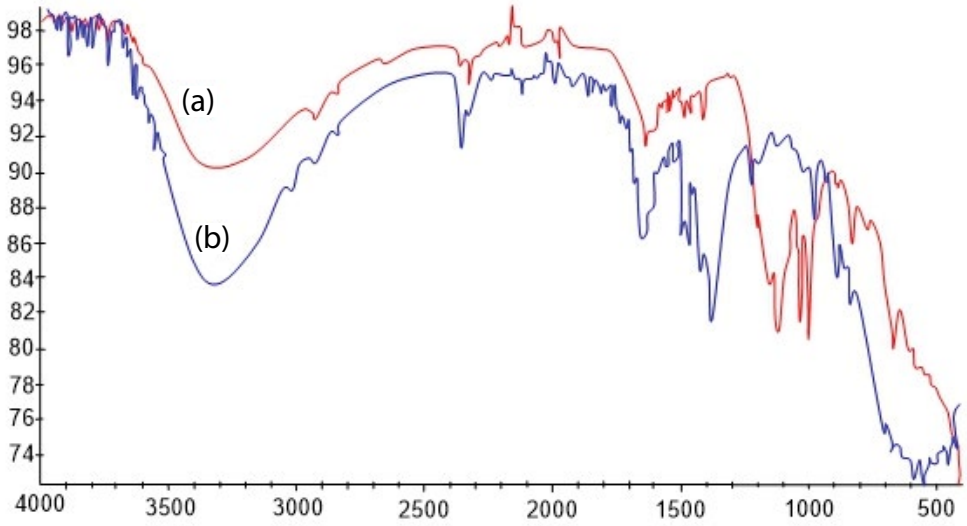

Fig. 2. (a) FT-IR of Amberlite MB9L and (b) FT-IR of modified resin.

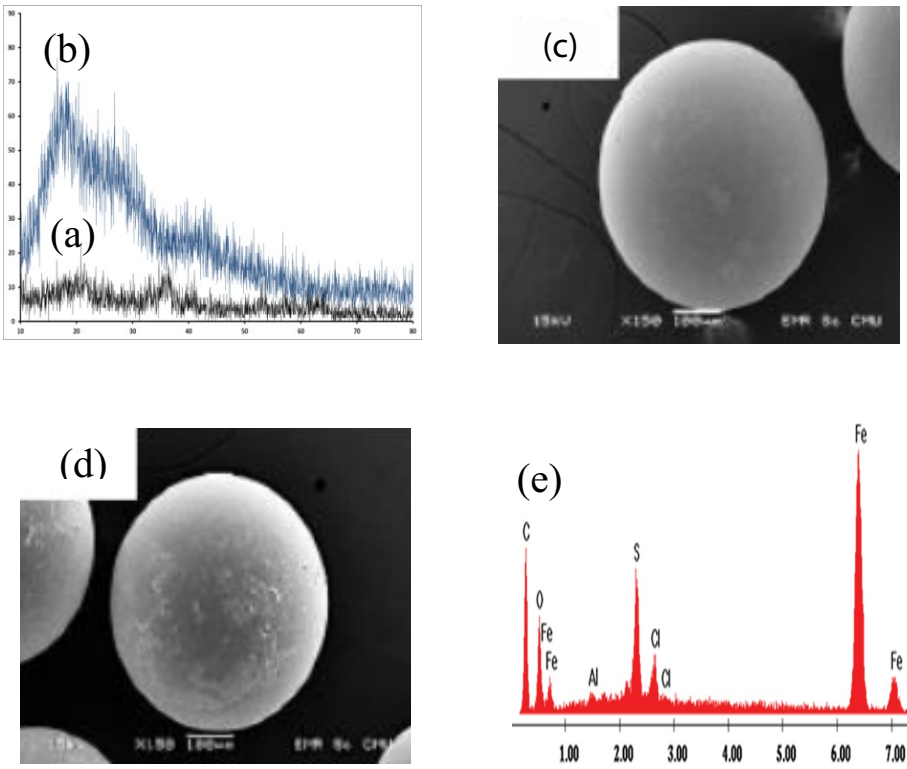

Fig. 3. (a) XRD of Amberlite MB9L, (b) XRD of modified resin, (c) SEM of Amberlite MB9L, (d) SEM of modified resin, and (e) EDX of modified resin.

and smooth surface, while the surface of FO-Amberlite (Fig. 3d) showed roughness due to the deposition of iron oxide particles. The EDX analysis modified resin illustrated in Fig. 3e. It can be revealed that Amberlite resin contained mainly of carbon and chlorine which may result from the polymeric matrix and exchangeable ion of the resin composition. Meanwhile, Fe element was detected in the elemental compositions of modified resin. This confirmed that the loading of iron oxide onto resin is successful.

3.2. Factors affecting removal of PO_4^{-3} ions

The optimal conditions for phosphate adsorption on FO-Amberlite adsorbents were evaluated by varying some factors as follow:

3.2.1. Effect of dose

Standard phosphate solution was prepared (10 ppm), then different amounts of the modified Amberlite resin

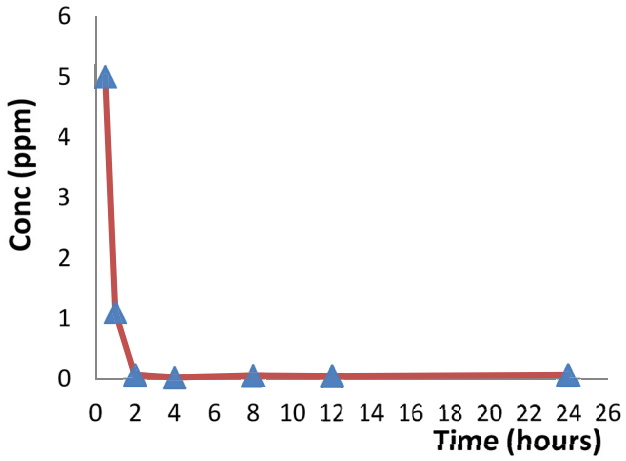

Fig. 4. Effect of time.

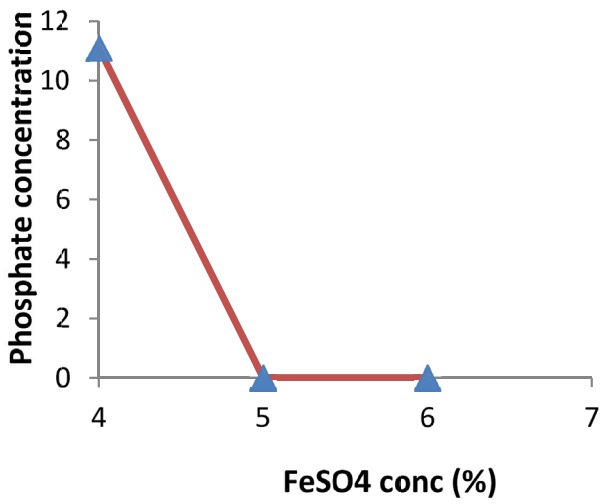

Fig. 5. Effect of $FeSO_4$ concentration.

were added to a phosphate-containing solution with resin/solution ratios of (5, 10, and 15 g/L). The optimum result was observed when 10 g of resin was immersed in a solution containing 10 ppm of phosphate, where the phosphate concentration decreased from 10 to 0.003 ppm.

3.2.2. Effect of adsorption time

The modified Amberlite resin was further challenged with time. 5 g of resin was immersed in a solution containing 55 ppm phosphate at different times (0.5, 1, 2, 4, 8, 12, and 24 h). The results showed that phosphate concentration is significantly decreasing until it almost reaches near-zero concentration after 2 h. Fig. 4 shows that there is a definite time at which complete phosphate removal occurs after this time desorption of phosphate ions in the solution will occur.

3.2.3. Effect of NaOH washing

As previously mentioned in this paper that the modified resin should be washed with a sodium hydroxide solution to remove the excess sulfate leachate into the treated water. Different concentrations of NaOH solution were prepared (0.01, 0.1, and 0.5 M) to define the best-suited concentration at which most of the sulfate ions will be removed. The highest amount of sulfate removed was recorded when 0.5 M of NaOH was used. It should be noted that washing with NaOH solution is a good way for sulfate removal but at definite concentration. Reviewing the literature, it was found that adding 2 N sodium hydroxide solution cannot separate sulfate ions [21].

3.2.4. Effect of $FeSO_4$

The selectivity toward phosphate was improved by introducing ferric oxide nanoparticles into the resin. Therefore, the resin was modified by treating it with a ferrous sulfate solution. Different concentrations of ferrous sulfate solution were prepared to show the effect of concentration change on removing phosphate from polluted water. Three solutions of $FeSO_4$ (4%, 5%, and 6% wt./v) were used in the modification process, then the modified resins were challenged with a naturally-occurring water sample having 12.88 ppm phosphate. It was found that the efficiency of the modified resin increased as the concentration of ferrous sulfate increased. However, it requires much more washing with NaOH solution to remove the excess sulfate, (Fig. 5). The increase in the adsorption capacity as the iron ion concentration increase could be attributed to the availability of a higher amount of adsorption sites onto anion resin surface, resulting in an enhancement of the phosphate adsorption. The maximum adsorption capacity was obtained at a 6% $FeSO_4$ solution with NaOH washing. The drop in the adsorption capacity due to further increase of iron concentration is probably referred to as the pore blockage and self-aggregation of iron oxide particles at a high amount of iron. This may reduce the available active sites for adsorption and hinder the diffusion of phosphate into the adsorption sites of adsorbent, lowering the adsorption capacity [22,23].

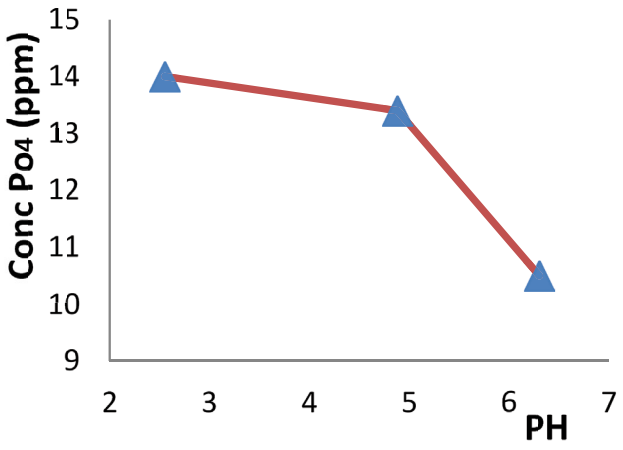

Fig. 6. Effect of PH.

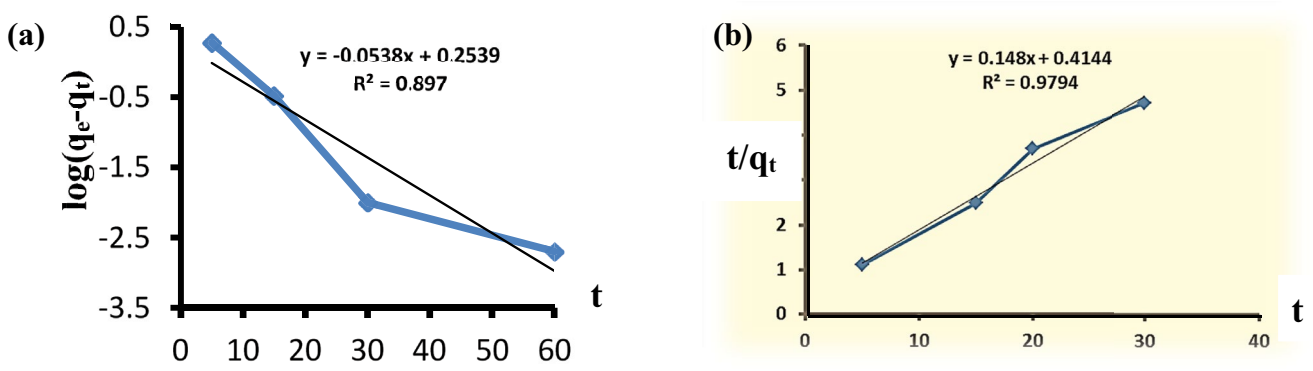

Fig. 7. (a) Pseudo-first-order model and (b) pseudo-second-order model.

3.2.5. Effect of pH

The modified Amberlite was prepared at different pH values and then mixed with another water sample containing 81 ppm phosphate. As shown in Fig. 6, it was shown that as the pH values increase, the removal capability of phosphate ions increases. The maximum phosphate sorption occurs in the PH range of 6.0–8.0. Since the pH of typical secondary wastewaters is in the vicinity of 7.0, phosphate removal by HAIX does not warrant any pH adjustment [12].

3.3. Adsorption kinetic models

The pseudo-first-order kinetic model [24] and pseudo-second-order kinetic model [25] were employed to fit the experimental data and to understand the adsorption mechanism of PO_4^{3-} ions using modified resin adsorbent. The Eq. (3) of the pseudo-first-order kinetic model is as follows:

$$\log\left(q_e - q_t\right) = \log q_e - k_1 t \tag{3}$$

where q_e and q_t (mg/g) are the adsorption capacities at equilibrium time and time t, respectively. k_1 (l/min) is the pseudo-first-order rate constant. From plotting $\log(q_e - q_t)$ vs. t (Fig. 7a), k_1 and q_e can be obtained from the slope and intercept, respectively. The Eq. (4) of the pseudo-second-order kinetic model is as follows:

$$\frac{t}{q_t} = \frac{1}{k_2 q_e^2} + t q_e \tag{4}$$

where k_2 [g/(mg min)] is the pseudo-second-order rate constant. From plotting t/q_t vs. t (Fig. 7b), the values of q_e and k_2 can be obtained from the slope and intercept, respectively. From the figures, it was observed that the values of R^2 of the pseudo-first-order kinetic model were better than the other two models. Therefore it's more applicable to the kinetics adsorption of PO_4^{-3} ions and therefore suggests a chemisorption process.

4. Adsorption mechanism

It is known that Amberlite resin has an affinity for all anions and cations with no selectivity. After modification with Fe it was able to efficiently adsorb phosphate ions even in the presence of chloride and sulfate ions. This may be due to formation of inner complex, monovalent and divalent phosphate ($H_2PO_4^-$ and HPO_4^{2-}, respectively) ions onto HFO surface sites. Contrary, sulfate, and chloride form only outer-sphere complexes through coulombic interaction, and hence, they are less selectively bound to the resin exchanger [12].

5. Conclusion

The ion exchange system is a good system for pollutant removal with no selectivity. Commercially available ion exchangers are robust and durable but exhibit poor selectivity. Conversely, HFO particles have high phosphate sorption affinity but lack mechanical strength for prolonged usage in fixed-bed columns. This investigation presents the development of selectivity of ion exchange resin by adding nano metal oxide to the ion exchange resin. Adding nano metal oxides to the resin increase the selectivity of the resin, for example, modification of Amberlite resin with nano iron oxide increases its selectivity for phosphate removal.

References

[1] M.A. Ahmed, Z.M. Abou-Gamra, H.A.A. Medien, M.A. Hamza, Effect of porphyrin on photocatalytic activity of TiO_2 nanoparticles toward Rhodamine B photodegradation, J. Photochem. Photobiol., B, 176 (2017) 25–35.
[2] A.D. Kney, B. Dreibelbis, D. Zhao, A.K.Sengupta, A pilot Study Phosphate and Nitrate Removal from Treated Domestic Wastewater using Unique Enhanced Ion Exchange Process, CSCE/EWRI of ASCE Environmental Engineering Conference, Niagara Falls, ON, 2002.
[3] A.K. Sengupta, D. Zhao, Selective Removal of Phosphate and Chromate by Ion Exchangers, US Patent 6136199, 2000.
[4] D. Zhao, A.K. Sengupta, Y. Zhu, Trace contaminants sorption through polymeric ligand exchange, Ind. Eng. Chem. Res., 34 (1995) 2676–2684.
[5] D. Zhao, A.K. Sengupta, Ultimate removal of phosphate using a new class of anion exchanger, Water Res., 32 (1998) 1613–1625.
[6] S. Tanada, M. Kabayama, N. Kawasaki, T. Sakiyama, T. Nakamura, M. Araki, T. Tamura, Removal of phosphate by aluminum oxide hydroxide, J. Colloid Interface Sci., 257 (2003) 135–140.
[7] W. Stumm, J.J. Morgan, Aquatic Chemistry: Chemical Equilibria and Rates in Natural Waters, Wiley, New York, 1995.
[8] D.A. Dzombak, F.M.M. Morel, Surface Complexation Modeling: Hydrous Ferric Oxide, Wiley, New York, 1990.

[9] T.M. Suzuki, J.O. Bomani, H. Matsunaga, Y. Yokoyama, Preparation of porous resin loaded with crystalline hydrous zirconium oxide and its application to the removal of arsenic, React. Funct. Polym., 43 (2000) 165–172.
[10] P.K. Dutta, A.K. Ray, V.K. Sharma, F.J. Millero, Adsorption of arsenate and arsenite on titanium dioxide suspensions, J. Colloid Interface Sci., 278 (2004) 270–275.
[11] L. Cumbal, A.K. Sengupta, Arsenic removal using polymer-supported hydrated iron(III) oxide nanoparticles: role of Donnan membrane effect, Environ. Sci. Technol., 39 (2005) 6508–6515.
[12] M. Lee Blaney, S. Cinar, A.K. Sengupta, Hybrid anion exchanger for trace phosphate removal from water and wastewater, Water Res., 41 (2007) 1603–1613.
[13] A.K. Sengupta, L. Cumbal, Method of Manufacture and Use of Hybrid Anion Exchanger for Selective Removal of Contaminating Ligands from Fluids, U.S. Patent No. 7,291,578, U.S. Patent and Trademark Office, Washington, DC, 2005.
[14] D. Kauspediene, E. Kazlauskiene, R. Cesuniene, A. Gefeniene, R. Ragauskas, A. Selskiene, Removal of the phthalocyanine dye from acidic solutions using resin with the polystyrene divinylbenzene matrix, Chemija, 24 (2013) 171–181.
[15] S. Ghosh, K.J. Dhole, M.K. Tripathy, R. Kumar, R.S. Sharma, FT-IR spectroscopy in the characterization of the mixture of nuclear grade cation and anion exchange resins, J. Radioanal. Nucl. Chem., 304 (2015) 917–923.
[16] S.M. Alshehri, M. Naushad, T. Ahamad, Z.A. Alothman, A. Aldalbahi, Synthesis, characterization of curcumin based eco-friendly antimicrobial bio-adsorbent for the removal of phenol from aqueous medium, Chem. Eng. J., 254 (2014) 181–189.
[17] Q. Zhou, X. Wang, J.Y. Liu, L. Zhang, Phosphorus removal from wastewater using nano-particulates of hydrated ferric oxide doped activated carbon fiber prepared by sol–gel method, Chem. Eng. J., 200 (2012) 619–626.
[18] G. Unsoy, S. Yalcin, R. Khodadust, G. Gunduz, U. Gundus, Synthesis optimization and characterization of chitosan-coated iron oxide nanoparticles produced for biomedical applications, J. Nanopart. Res., 14 (2012) 964.
[19] Y.-C. Chang, D.-H. Chen, Preparation and adsorption properties of monodisperse chitosan-bound Fe_3O_4 magnetic nanoparticles for removal of Cu(II) ions, J. Colloid Interface Sci., 283 (2005) 446–451.
[20] H. Li, Z. Li, T. Liu, X. Xiao, Z. Peng, L. Deng, A novel technology for biosorption and recovery hexavalent chromium in wastewater by bio-functional magnetic beads, Bioresour. Technol., 99 (2008) 6271–6279.
[21] D.D.T. Rathnayaka, Development of a process to manufacture high-quality refined salt from crude solar salt, Int. J. Chem. Mol. Nucl. Mater. Metall. Eng., 7 (2014) 1009–1014.
[22] N. Zhang, L.S. Lin, D. Gang, Adsorptive selenite removal from water using iron-coated GAC adsorbents, Water Res., 42 (2008) 3809–3816.
[23] L.T. Mayo, C. Yavuz, S. Yean, L. Cong, H. Shipley, W. Yu, J. Falkner, A. Kan, M. Tomson, V.L. Colvin, The effect of nanocrystalline magnetite size on arsenic removal, Sci. Technol. Adv. Mater., 8 (2007) 71–75.
[24] S. Lagergren, Zur Theorie der sogenannten Absorption gelöster Stoffe, PA Norstedt & söner, 1898.
[25] Y.S. Ho, G. McKay, Pseudo-second-order model for sorption processes, Process Biochem., 34 (1999) 451–465.